Asian Journal of Chemistry; Vol. 27, No. 12 (2015), 4634-4640

ASIAN JOURNAL OF CHEMISTRY

http://dx.doi.org/10.14233/ajchem.2015.19293

Design, Molecular Docking Study and Synthesis of 3,6-*Bis*(3'-substituted propoxy)xanthone Derivatives as COX-2 Inhibitors

BRAJESH SHANKAR[1], APAROOP DAS[2] and PRATAP PARIDA[3,*]

[1]Department of Pharmaceutical Sciences, Sardar Bhagwan Singh Postgraduate Institute of Biomedical Sciences & Research, Dehradun-248 161, India
[2]Department of Pharmaceutical Sciences, Dibrugarh University, Dibrugarh-786 004, India
[3]Centre for Studies in Biotechnology, Dibrugarh University, Dibrugarh-786 004, India

*Corresponding author: E-mail: pratapparida2007yahoo.com@gmail.com

Received: 27 April 2015; *Accepted*: 27 June 2015; *Published online*: 29 August 2015; AJC-17521

New drug discovery is considered broadly in terms of two kinds of investigational activities such as exploration and exploitation. Docking of small molecules in the receptor binding site and estimation of binding affinity of the complex is a vital part of structure based drug design. The current study deals with the evaluation of cyclooxygenase (COX) inhibitory activity of xanthone using *in silico* docking studies. *In silico* docking studies were carried out using AutoDock 4.2, based on the Lamarckian genetic algorithm principle. Molecular properties of the ligands were investigated by using Discovery Studio 3.1. The docking results showed that all the selected xanthone derivatives having binding energy ranging between -6.61 to -15.46 kcal/mol when compared with that of the standard drug *i.e.* celecoxib (-9.94 kcal/mol). All the 3,6-*bis*(3'-substituted propoxy)xanthone derivatives contributed cyclooxygenase inhibitory activity because of its structural parameters. Molecular docking analysis of these compounds can lead to further development of potent cyclooxygenase inhibitors for the treatment of inflammation. A further structure-based research methodology of virtual screening was employed to analyze the selectivity of the 2 isozymes. After docking study these derivatives were successfully synthesized.

Keywords: Molecular docking, Structure activity relationship, Synthesis, Topo isomerase, Xanthone derivatives.

INTRODUCTION

Prostaglandins are converted into arachdonic acid by prostaglandin endoperoxide hydroxysynthases (PGHS). Two main isoform PGHS-1 and PGHS-2, were referred to as COX-1 (cyclooxygenase-1) and COX-2, respectively[1]. The predominantly constitutive form of the enzyme COX-1, is expressed throughout the body and performs a number of homeostatic functions, whereas COX-2 is induced by cytokines or antigens[2,3]. Cyclooxygenase-1 (COX-1) is involved in gastric mucosa protection, platelet aggregation, ovary and breast cell carcinoma develop-ment and renal blood regulation[4]. In contrast, the inducible form, COX-2 is expressed in response to inflammation and is involved in the production of the prostaglandins that mediate pain and support the inflammatory process[5]. The pain caused by inflammation is treated by COX-2 inhibition[6]. In addition, COX-2 mediating the vessel formation and proliferation plays a crucial role in tumorigenesis[7]. All the classic NSAIDs (non-steroidal anti-inflammatory drugs) inhibit both COX-1 and COX-2 at standard anti-inflammatory doses. Therefore, molecular-based targeting strategies were employed to develop specific COX-2 inhibitors to circumvent the gastric and renal toxicities caused by mixed COX inhibitors[8-10]. Investigations of many naturally occurring xanthones as well as their synthetic derivatives, show broad spectrum of anti-inflammatory activity[11]. The present research work was based on *in silico* docking and to synthesize 3,6-*bis*(3'-substituted propoxy)-xanthone derivatives the substitution is made on 3- and 6-position by propane side chain with different nucleophiles to obtain a series of new xanthone derivatives. Docking is done by autodock 4.2 to the active site of the COX-2. The structures of the synthesized compounds were confirmed on the basis of analytical and spectral data.

EXPERIMENTAL

Retrieval of 3D structure: The 3D structure of the protein was downloaded from Research Collaboratory for Structural Bioinformatics (RCSB), Protein Databank (PDB, http://www.pdb.org). The PDB ID of the selected protein was found to be 3LN1.

Ligand preparation and optimization: The ligands were drawn using Moldraw tool of Exome™ Horizon in 2D and were converted into 3D before submission for docking. The

general structure was given in the Fig 1. The ligands optimization was performed using ADMET module of Accelrys Discovery studio 3.1.

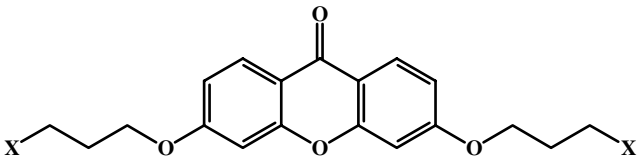

Fig. 1. General structure of the proposed compounds

Ligand structure preparation, toxicity and drug likeness: The data set of different 3,6-*bis*(3'-substituted propoxy)xanthone derivatives, were generated ligand molecules. ChemAxon is a freeware which developed by Advanced Chemistry Development, Inc. was used for drawing and conversion of 2D chemical structure of compound to 3D structures. It was also used for optimization of the ligand molecules. Medchem Designer was used for ADME/Tox screening of the selected ligands and the results were recorded. *In silico* prediction biological activity of the compounds were calculated such as molecular weight, hydrogen bond donors/acceptors, log P and total polar surface area (TPSA). Actelion (OSIRIS) [OSIRIS Property Explorer (http://wwworganic-chemistryorg/prog/peo/)] property explorer was used to screen the drug likeness. Toxicity risks were evaluated by calculating mutagenic, tumorigenic, irritant, reproductive effective, solubility, drug likeliness and drug score.

Docking methodology: The Lamarckian genetic algorithm (LGA) was employed for ligand conformational searching, which is a hybrid of a genetic algorithm and a local search algorithm. This algorithm first builds a population of individuals (genes), each being a different random conformation of the docked molecule. Each individual is then mutated to acquire a slightly different translation and rotation and the local search algorithm then performs energy minimizations on a user-specified proportion of the population of individuals. The individuals with the low resulting energy are transferred to the next generation and the process is then repeated. Rapid energy evaluation was achieved by precalculating atomic affinity potentials for each atom in the ligand molecule. In the AutoGrid procedure, the target enzyme was embedded on a three dimensional grid point[12]. The energy of interaction of each atom in the ligand was encountered. AutoDock was run several times to get various docked conformations and used to analyze the predicted docking energy. The binding sites for these molecules were selected based on the ligand-binding pocket of the templates[13]. AutoDock Tools provide various methods to analyze the results of docking simulations such as, conformational similarity, visualizing the binding site and its energy and other parameters like intermolecular energy and inhibition constant. For each ligand, ten best poses were generated and scored using AutoDock 4.2 scoring functions[14]. The analogues were docked into the binding pocket. The similarity of docked structures is measured by computing the root-mean-square deviation (RMSD) between the coordinates of selected molecular conformation with the molecular conformation having lowest interaction energy which is ranked on top. Clusters are created based on the comparison of conformations using RMSD values.

Synthesis: Synthesis of all the designed compounds (**B1-B9**) involves three steps reactions. All the targeted compounds were synthesized using laboratory grade chemicals and solvents without further purification. Eaton's reagent was prepared by dissolving phosphorus pentoxide in methane sulphonic acid in 1:10 ratio *i.e.* 10 g phosphorus pentoxide was dissolved in 100 mL methane sulphonic acid. 100 mL of Eaton's reagent was added slowly to a mixture of resorcinol (60 mmol) and 2,4-dihydroxybenzoic acid (60 mmol). The mixture was warmed up to 70 °C for 35 min under stirred. Then cooled to room temperature and the reaction was poured into an ice bath and stirred for 2 h. The resulting solid collected by filtration, washed with water until pH 6 and dried at 60 °C. Potassium carbonate (0.25 mmol) was added to a solution of 3,6-*bis*(3'-substituted propoxy)xanthone (0.2 mmol) and 1,3-dibromopropane in acetone. The mixture was refluxed under stirring for 24 h at 65 °C. Cooled the mixture, filtered and concentrated the filtrate to obtain crude product. 3,6-*bis*(3'-substituted propoxy)xanthone (10 mmol) and selected amine (20 mmol) was dissolved in 20 mL of acetone and stirred at room temperature for 48 h (**Scheme-I**). The end of reaction was confirmed by TLC with the formation of only one spot. The crude product was purified[14-17].

Spectral data

3,6-*Bis*[3-(3-nitrophenylamino)propoxy]xanthone (B1): UV-visible spectrum (λ_{max}): 554 nm (DMSO); FT-IR (KBr pellets, ν_{max}, cm^{-1}): 3431.36 (2°amine), 2845.30 (C-C str., alkyl), 1346.31 (C-N str., nitro compound), 1579.70 (N-H benzene, 2°amine), 1622.13 (C=O str., Keto group), 1430 (C-C str., aromatic); ^{1}H NMR δ: 3.436 (m, 2H, -$CH_2CH_2CH_2$-NH-aromatic), 1.98 (t, 2H, -CH_2CH_2-NH- aromatic), 3.03 (m, 2H, -CH_2-NH-aromatic), 1.983 (m, 1H, -NH aromatic), 6.768 (m, 3H-xanthone); ^{13}C NMR δ: 63.188 (-$CH_2CH_2CH_2$-NH-phenyl), 130 (4a, 4b xanthone), 149 (C=O xanthone), 130 (2C-phenyl); 40.004 (-CH_2-NH-phenyl); MS *m/z* (%): 586 (7.7 %), [M^+].

3,6-*Bis*[3-(4-nitrophenylamino)propoxy]xanthone (B2): UV-visible spectrum (λ_{max}): 556 nm (DMSO); IR (KBr pellets, ν_{max}, cm^{-1}): 3481.51 (2°amine), 2800.32 (CH str., alkyl), 1631.78 (C=O str., keto group), 1475.54 (C-C str., aromatic), 1307.74 (C-N str., nitro compound), 1595.13 (N-H ben., 2°amine) ^{1}H NMR δ: 1.28 (m, 2H, 6.8, -$CH_2CH_2CH_2$-NH-phenyl), 1.52 (m, 2H, -CH_2CH_2-NH-phenyl), 3.28 (t, 2H, -CH_2-NH-phenyl), 6.69 (d, 2H, 2-H-phenyl), 7.26 (t, 1H, 6-H-xanthone), 7.69 (d, 1H, 8-H-xanthone); ^{13}C NMR δ: 24.01 (-$CH_2CH_2CH_2$ NH-phenyl-), 27.48 (-CH_2CH_2 NH-phenyl), 31.69 (-CH_2 NH-phenyl), 112.58 (2-C-phenyl), 117.29 (5-C-xanthone), 119.33 (5-C-phenyl, 7-C-xanthone), 129.75 (8-C-xanthone), 135.63 (4-C-phenyl), 155.62 (4a, 4b-C-xanthone), 160.20 (1, 3-C-xanthone); MS *m/z* (%): 585 (34.2 %), [M^+].

3,6-[3-(2-Hydroxyphenylamino)propoxy]xanthone (B3): UV-visible spectrum (λ_{max}): 524 nm (DMSO); IR (KBr pellets, ν_{max}, cm^{-1}): 3070 (2°amine), 1604.77 (C=O str., keto group), 1431.18 (C-C str., aromatic), 1309.67 (OH ben., phenolic), 1502.55 (N-H ben., 2°amine); ^{1}H NMR δ: 1.37 (m, 2H, -$CH_2CH_2CH_2$-NH-phenyl), 5.87 (s, 1H, 2-H-phenyl), 6.06

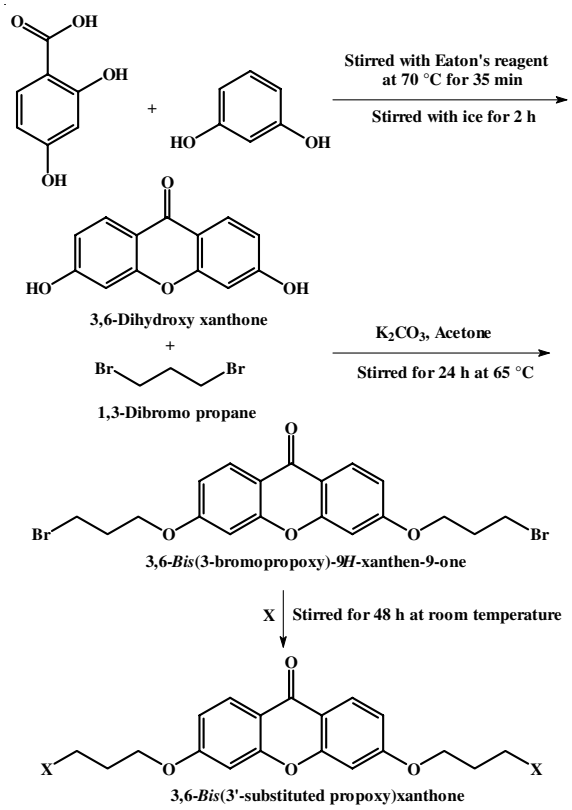

Scheme-I

(s, 1H, 2-H-xanthone), 6.11 (d, 1H, 6-H-phenyl), 6.17 (s, 1H, 4-H-xanthone), 7.12 (d, 1H, 5-H-xanthone), 7.16 (t, 1H, 7-H-xanthone), 7.67 (d, 1H, 8-H-xanthone); ^{13}C NMR δ: 92.50 (2-C-xanthone), 5-C-xanthone), 120.17 (7-C-xanthone), 129.99 (8-C-xanthone), 135.57 (6-C-xanthone), 157.12 (4a, s4b-C-xanthone), 162.50 (1,3-C-xanthone), 171.78 (9-C-xanthone), 39.693 (-$CH_2CH_2CH_2$NH-phenyl). MS *m/z* (%): 529 (34.1); [M$^+$].

3,6-*Bis*[3-(ethyl(phenyl)propoxy]xanthone (B4): UV-visible spectrum (λ_{max}): 534 nm (DMSO); IR (KBr pellets, ν_{max}, cm^{-1}): 2927.94 (C-H str., alkyl), 1604.77 (C=O, keto group), 1463.97 (C-C str., aromatic) 1346.31 (C-N str., 3° amine); ^{1}H NMR δ: 4.129 (d, 2H, -$CH_2CH_2CH_2$-N-ethylaniline), 8.63 (d, 2H, -CH_2CH_2-N-ethylaniline), 1.252 (d, 3H, CH_3CH_2-3°amine phenyl), 1.785 (s, 1H, 2Hphenyl), 7.309 (d, 1H, 8Hxanthone), 3.343 (s, 3H, -CH_2-3°aminephenyl); ^{13}C NMR 65.734 (3C, methylphenyl), 162.673 (4a, 4b, phenyl)115.021 (2C, phenyl); 129.459 (3C-phenyl); MS *m/z* (%) : 538 (100); [M$^+$].

3-[5-(Furan-2-ylmethylamino)propoxy]hydroxy-xanthone (B5): UV-visible spectrum (λ_{max}): 537 nm (DMSO). FT-IR spectrum (KBr pellets, ν_{max}, cm^{-1}): 3143.97 (N-H str., 2°amine); 2800 (C-H str., alkyl); 1604.77 (C=O str., keto group); 1465.90 (C-C str., aromatic). NMR spectrum: ^{1}H NMR (400 MHz, D_2O): δ 4,098 (s, 2H, -$CH_2CH_2CH_2$-NH-furfuryl); 1.942 (s, 2H, -CH_2CH_2-NH-furfuryl); 4.334 (s, 1H, -NH-furfuryl); 1.99 (s, 1H, 2H furan); 7.652 (d, 1H, 8H, xanthone); 6.503 (t, 1H, 1H xanthone). ^{13}C NMR (100 MHz, D_2O): δ 65.930 (3C, furfuryl); 62.795 (4C-furan); 98.909 (1C furan); 158 (4a, 4b xanthone); 169.228 (C=O xanthone). Mass spectrum *m/z* (%) : 500.28 (5.9); [M$^+$].

3,6-*Bis*[3-(cyclohexylamino)propoxy]xanthone (B6): UV-visible spectrum (λ_{max}): 563 nm (DMSO). FT-IR spectrum (KBr pellets, ν_{max}, cm^{-1}): 3045.60 (N-H str., 2°amine); 2970.38 (C-H str., alkyl); 1608.63 (C=O str., keto group); 1130.29 (C-O str., alkyl ether); 1469.76 (C-C str., aromatic). NMR spectrum: ^{1}H NMR (DMSO-d_6): 3.875 (s, 2H, -$CH_2CH_2CH_2$-NH-cyclohexyl); 1.641 (s, 2H, -CH_2CH_2-NH-cyclohexyl); 2.072 (d, 1H, NH cyclohexyl); 7.505 (d, 1H, 6H xanthone); 1.44 (s, 1H, cyclohexyl). ^{13}C NMR (DMSO-d_6): δ 23.20 (3-C-propane); 27.48 (2-C-propane); 38.75 (2-C-cyclohexyl); 64.83 (1-C-propane); 117.36 (5-C-xanthone); 120.27 (7-C-xanthone); 129.98 (8-C-xanthone); 131.43 (6-C-xanthone); 162.50 (1-C-xanthone). Mass spectrum *m/z* (%): 503 (5.7); [M$^+$].

3,6-*Bis*(3'-indole propoxy)xanthone (B7): UV-visible spectrum (λ_{max}): 345 nm (methanol); FT-IR spectrum (KBr pellets, ν_{max}, cm^{-1}): 3047 (C-H str., aromatic); 2926 (C-H str., alkyl); 1334 (C-N str., 3°amine); 1488 (C-C str., aromatic); 1105 (C-O str., 6 membered cyclic ether)NMR spectrum: ^{1}H NMR (MeOD): δ 6.417-6.425 (d, 1H, xanthone, H-1 & H-8, *J* = 3.2 Hz); 6.291-6.317 (t, 1H, xanthone, *J* = 8.4 Hz, *J* = 2 Hz); 3.312-3.574 (t, 2H, H-3', *J* = 6.4 Hz); 4.100-4.114 (d, 2H, H-1' *J* = 5.6 Hz); 6.964-7.001 (t, 1H, indole, H-5, *J* = 7.2 Hz, *J* = 7.6 Hz); 7.520-7.538 (d, 1H, indole, H-2, *J* =7.2 Hz); 7.195-7.202 (d, 1H, indole, H-3, *J* = 2.8 Hz); 7.056- 7.094 (t, 1H, indole, H-6, *J* = 8.00 Hz, *J* =7.2); 7.324-7.375 (m, 1H, indole, H-4 & H-7); ^{13}C NMR (MeOD): δ 199.47 (C-9, xanthone); 164.56 (C-1 and C-8); 168.61 (C-3 and C-6); 137.63 (C-5a & C-4a); 112.11 (C-2 and C-7); 104.64 (C-8a and C-9a); 122.47 (C-4 and C-5); 125.46 (C-2, indole); 102.24 (C-3, indole); 119.97 (C-4, indole); 121.16 (C-5, indole); 114.19 (C-6, indloe); 110.61 (C-7, indole); 135.50 (C-7a, indole); 129.11 (C-3a); 49.69 (C-1'); 49.49 (C-3'); 48.41 (C-2'); Mass spectrum *m/z* (%): 543 (38.7); [M$^+$].

3,6-*Bis*(3'-*p*-aminoacetophenone propoxy)xanthone (B8): UV-visible spectrum (λ_{max}): 318 nm (methanol). FT-IR spectrum (KBr pellets, ν_{max}, cm^{-1}): 3391 (N-H str., 2°amine); 2921 (C-H str., alkyl); 1630 (C=O str., keto group); 1487 (C-C str., aromatic); 1338 (C-N str., 2°amine); 1586 (N-H ben., 2°amine); 1100 (C-O str., 6 membered cyclic ether).NMR spectrum: ^{1}H NMR (MeOD): δ 3.175 (s, 1H, N-H); 2.309 (s, 3H, CH_3); 4.878 (s, 2H, H-3'); 7.592-7.613 (d, 1H, benzene, H-3 and H-5, *J* = 8.4 Hz); 7.171-7.193 (d, 1H, benzene, H-2 and H-6, *J* = 8.8 Hz); 6.476-6.497 (d, 1H, xanthone, H-1 and H-8, *J* = 8.4 Hz); 6.123-6.162 (m, 1H, xanthone). ^{13}C NMR (MeOD): δ 199.37 (C-9); 199.11 (C=O); 135.49 (C-1, benzene); 132.21 (C-4, benzene); 126.85 (C-2 & C-6, benzene); 169.45 (C-3 & C-6); 164.65 (C-1 & C-8); 114.51 (C-3 & C-5, benzene); 110.40 (C-2 & C-7); 104.82 (C-8a & C-9a); 155.38 (C-4a & C-5a); 113.51 (C-4 & C-5); 25.95 (CH_3); 49.70 (C-1'); 49.50 (C-3'); 48.44 (C-2'). Mass spectrum *m/z* (%): 580 (8.4); [M$^+$].

3,6-*Bis*(3'-*p*-aminobenzoic acid propoxy)xanthone (B9): UV-visible spectrum (λ_{max}): 346 nm (methanol). FT-IR spectrum (KBr pellets, ν_{max}, cm^{-1}): 3391 (N-H str., 2°amine); 2921 (C-H str., alkyl); 1630 (C=O str., keto group); 1487 (C-C str., aromatic); 1338 (C-N str., 2°amine); 1586 (N-H ben., 2°amine); 1100 (C-O str., 6 membered cyclic ether)NMR spectrum: ^{1}H NMR (MeOD): δ 7.758-7.777 (d, 1H, benzene, H-3 and H-5, *J* = 7.6 Hz); 7.322-7.343 (d, 1H, benzene, H-2 and H-6, *J* = 8.4 Hz); 6.640-6.661 (d, 1H, xanthone, H-1 and

H-8, *J*= 8.4 Hz); 6.312-6.336 (t, 1H, xanthone, *J* = 8.4 Hz, *J* = 2 Hz); 3.317 (s, 1H, N-H); 5.151-5.223 (d, 2H, H-3', *J* = 28.8 Hz). ^{13}C NMR (MeOD): δ 176.30 (COOH); 132.09 (C-1, benzene); 135.53 (C-4, benzene); 199.69 (C-9); 164.41 (C-1 and C-8); 168.20 (C-3 and C-6); 151.60 (C-5a and C-4a); 111.38 (C-2 and C-7); 104.66 (C- 8a and C-9a); 114.93 (C-4 and C-5); 49.75 (C-1'); 49.53 (C-3'); 49.33 (C-2').Mass spectrum *m/z* (%): 583 (36.7); [M$^+$].

RESULTS AND DISCUSSION

The water molecules and ligands attached to the protein were removed by using Swiss PDB Viewer. The Protein was having 552 number of groups, 8851 number of atoms and 8987 number of bonds. The binding site of the protein were analyzed and reported in Fig. 2. The molecular properties of all the derived groups (X) such as total polar surface area (TPSA), hydrogen bond donor (HBD), hydrogen bond acceptor (HBA), number of rotatable bonds (nRB) were provided in Table-1.

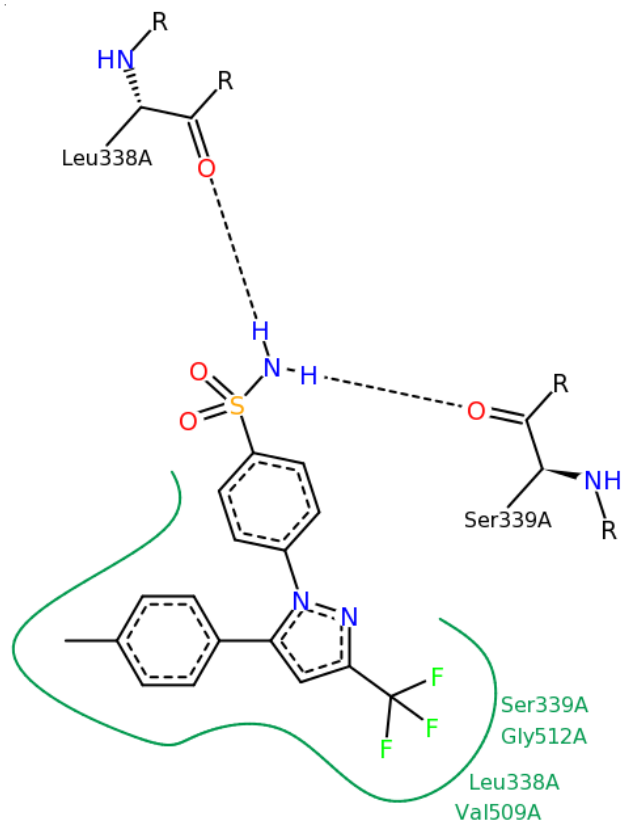

Fig. 2. Crystal structure of celecoxib bound at the COX-2 active site

Toxicity and drug likeness: The pharmacokinetics and pharmacodynamics properties of the ligands were calculated. The rotatable bonds, rigid bonds, flexibility, hydrogen bond donors, hydrogen bond acceptors, maximum rings, total charge, heavy atoms, hetero atoms, Lipinki's violation, oral bioavailability were calculated. The compounds successfully passed the Lipinkis rule. We observed that none of these compounds produce toxicity or mutagenicity. ADMET screening revealed that the ligands were non-toxic and passed Lipinski's rule and the Actelion property explorer revealed that ligands were non-mutagenic, non-tumorigenic and non-irritative with high solubility and drug likeness rule (Table-2).

Docking study: The ligands were targeted to celecoxib bound at the COX-2 active site. Here we observed that the residue Leu 338 and Ser 339 are inhibited by celecoxib. All the ligands successfully targeted to the active site of celecoxib. The binding energy was observed in the range of -6.61 to -15.46 kcal/mol. The binding energy of the selected ligands were plotted in the graph and from the graph (Fig. 3) the binding energy of all the ligands were observed among which the best ligand which shows better activity in all the active site was found to be **B1** (-15.46 kcal/mol). According to the active site analysis of celecoxib, it was observed that celecoxib formed two hydrogen bonds with the aminoacid residues Ser 339 and His 75 (Fig. 4). It also formed hydrophobic interaction with several amino acids however the active side residue Leu 338 was also inhibited with a hydrophobic bond by celecoxib (Fig. 4). The validation of residue inhibition to the active site of celecoxib was well observed by the xanthone derivatives. The ligand b1 formed six hydrogen bonds with the aminoacids. It was observed that, the residue Leu 338 and Ser 339 are inhibited properly (Fig. 5). The ligand b3 also interacted with the aminoacid Ser 339 (Fig. 6). Both the aminoacids are forming hydrophobic interaction with the ligand b5 (Fig. 7).

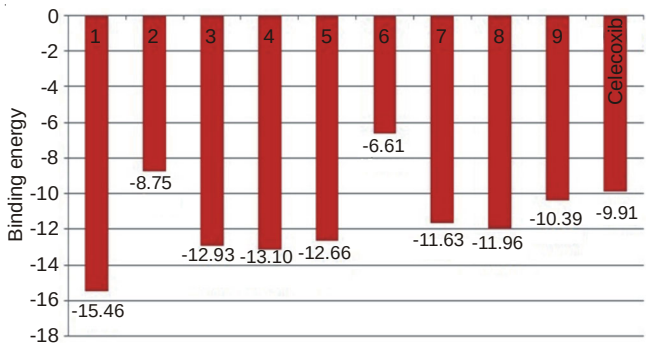

Fig. 3. Binding energy values for the proposed compounds (kcal/mol). The compound 1 (b1), 3 (b3), 4 (b4), 5 (b5) showed better binding energy than the control drug (celecoxib)

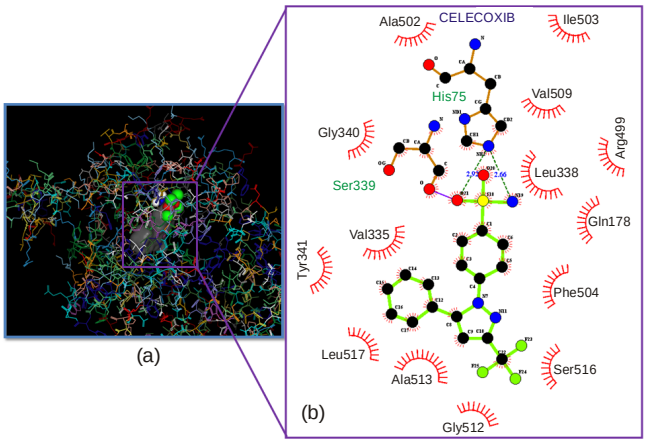

Fig. 4. (a) The binding site of the drug celecoxib in pharmacophore model. The green residues indicate lipophilic binding sites, the blue symbolizes the hydrogen bond donor, the red denotes hydrogen bond acceptor and the faded black directs the hydrogen residues. (b) The interacting amino acids with the protein. The green dotted line indicates the hydrogen bond formation and the rest are amino acids forming hydrophobic interaction

TABLE-1
CALCULATED MOLECULAR PROPERTIES OF THE COMPOUNDS

Ligand	Substituent (X)	m.w.	log P	Total polar surface area	Hydrogen bond acceptor	Hydrogen bond donor	Number of rotatable bonds
B1	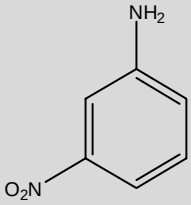	555.97	3.8	131.04	6	0	14
B2		555.97	3.8	131.04	6	0	14
B3	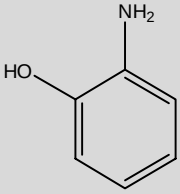	495.98	4.062	44.76	8	0	12
B4	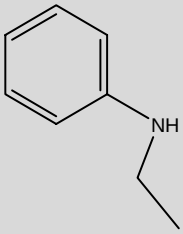	511.99	5.76	51.24	6	0	14
B5	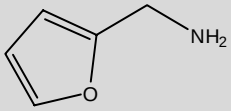	471.98	2.254	63.22	8	0	14
B6	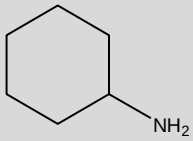	463.99	5.096	44.76	6	0	12
B7	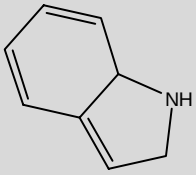	511.99	3.224	51.24	6	0	10
B8	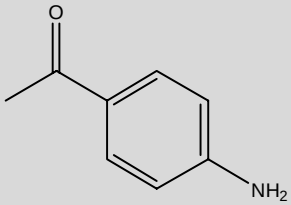	543.58	2.956	78.9	8	0	14
B9	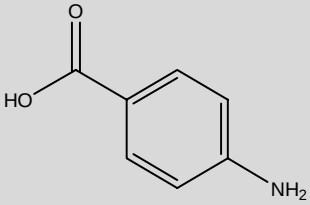	551.97	2.432	78.9	10	0	14

TABLE-2
c log P, SOLUBILITY, DRUG LIKENESS AND DRUG-SCORE ACCOUNTED BY OSIRIS PROPERTY EXPLORER

Ligand code	c log P	Solubility	Drug likeness	Drug-score
B1	3.32	-7.26	-4.16	0.1
B2	3.32	-7.26	-9.92	0.1
B3	4.47	-5.75	1.08	0.21
B4	6.47	-6.9	4.36	0.14
B5	2.35	-4.33	1.28	0.38
B6	4.86	-6.48	-4.09	0.11
B7	4.24	-4.57	3.54	0.31
B8	4.76	-6.47	-2.84	0.09
B9	1.95	-5.15	0.94	0.3
Celecoxib	2.24	-3.83	-7.03	0.39

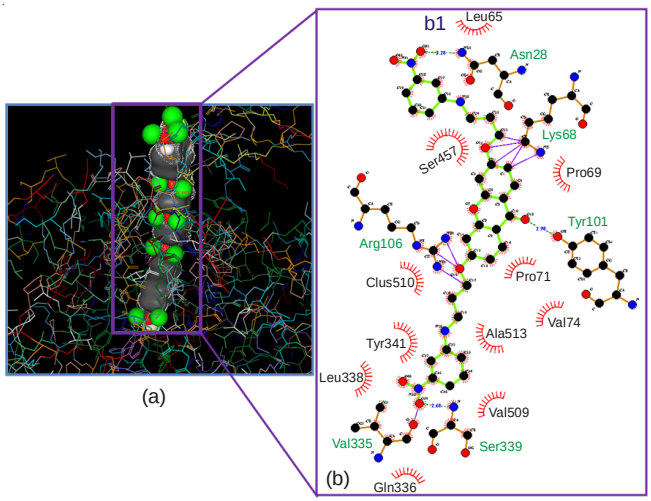

Fig. 5. (a) The binding site of the drug b1 in pharmacophore model. The green residues indicate lipophilic binding sites, the blue symbolizes the hydrogen bond donor, the red denotes hydrogen bond acceptor and the faded black directs the hydrogen residues. (b) The interacting amino acids with the protein. The green dotted line indicates the hydrogen bond formation and the rest are amino acids forming hydrophobic interaction

The physio-chemical properties of the synthesized compounds are given in Table-3.

Structure-activity correlation of the docked and synthesized compounds revealed some interesting assumptions. It was seen that the substitution of substituted primary or secondary aromatic amine into the 3rd and 6th position of the xanthone ring greatly enhances the PGHS-2 inhibitory activity. Electron withdrawing group (EWG) like NO_2 at *meta* position of aniline in ligand **B1** (binding energy:-15.46 kcal/mol) as the most active member of this study. NO_2 group is an EWG inductively

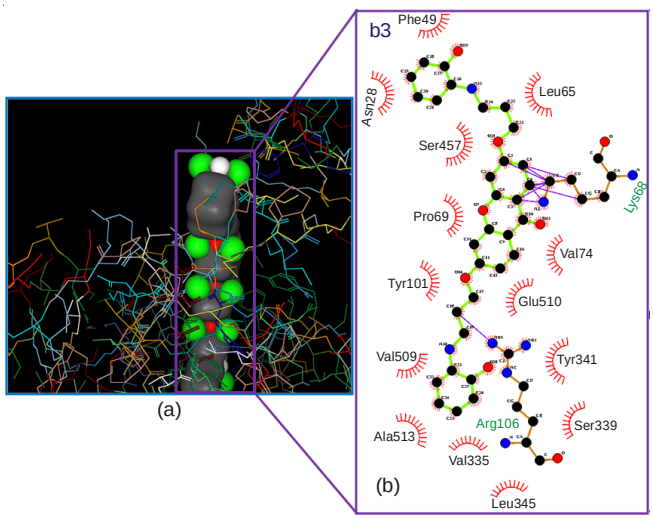

Fig. 6. (a) The binding site of the drug b3 in pharmacophore model. The green residues indicate lipophilic binding sites, the blue symbolizes the hydrogen bond donor, the red denotes hydrogen bond acceptor and the faded black directs the hydrogen residues. (b) The interacting amino acids with the protein. The green dotted line indicates the hydrogen bond formation and the rest are amino acids forming hydrophobic interaction

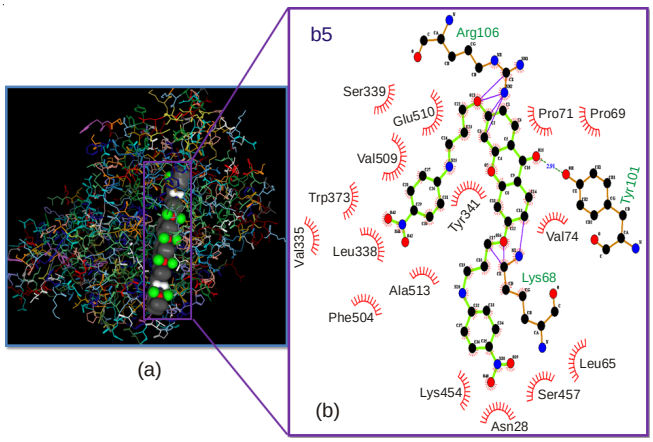

Fig. 7. (a) The binding site of the drug b5 in pharmacophore model. The green residues indicate lipophilic binding sites, the blue symbolizes the hydrogen bond donor, the red denotes hydrogen bond acceptor and the faded black directs the hydrogen residues. (b) The interacting amino acids with the protein. The green dotted line indicates the hydrogen bond formation and the rest are amino acids forming hydrophobic interaction.

as well as by resonance and so it is the strongest EWG reported. Besides EWG substituted on an aromatic ring is always *meta* directing and the NO_2 group in **B1** is in the *meta* position. This

TABLE-3
PHYSIO-CHEMICAL PROPERTIES OF THE SYNTHESIZED COMPOUNDS

Compound	State	Colour	Yield (%)	Solubility	m.p. (°C)
B1	Solid	Yellow	69.78	DMSO, methanol	160-165
B2	Solid	Light yellow	64.35	Acetone, ethanol, DMSO, methanol	140
B3	Solid	Brown	74.67	Methanol, DMSO	105-110
B4	Solid	Black	74.67	Chloroform, DMSO	110-120
B5	Solid	Black	71.23	DMSO, chloroform	178-180
B6	Solid	Light brown	77.47	Ethanol, DMSO	212-210
B7	Solid	Yellow	76.90	Ethanol, ethyl acetate, methanol and DMSO	160-165
B8	Solid	Yellow	71.00	Ethanol, ethyl acetate, methanol and DMSO	80-88
B9	Solid	Yellow	68.20	Ethanol, ethyl acetate, methanol and DMSO	190-195

corresponds to the higher activity of **B1** with respect to docking results of other ligands. On the other hand, EWG at *para* position of aniline in ligand **B2** produced lower binding energy (-8.75 kcal/mol). Interestingly, our study involved docking of only one ligand (**B6**) with an aliphatic ring cyclohexylamine but this compound showed the lowest binding energy (-6.61 kcal/mol) of all the nine ligands. Hence, aliphatic substitution in the xanthone nucleus may be considered to decrease the anti-inflammatory activity. N-substituted aniline in ligand **B4** also show relatively good binding energy (-13.10 kcal/mol). Electron donating group (EDG) at *ortho* position in substituent (**B3**) decreased the activity slightly and EWG at *para* position in substituent (**B9**) shows moderate binding efficacy. We currently all marketed NSAIDs are inhibitors of both COX-1 and COX-2.The aspect of enzyme selectivity of NSAIDs becomes important particularly under the point of view of low risk NSAIDs with reduced side-effects. Therefore, the classic NSAIDs are being pushed increasingly into the background, whereas selective COX-2 inhibitors with an attractive pharmacological profile and reduced side-effects are being favoured[5]. The clinical results for selective COX-2 inhibitors such as celecoxib and rofecoxib are promising. However, the tendency to search for more specific inhibitors has also provoked critical reactions. Moreover, the hormonal induction is important for ovulation and, at the end of pregnancy, high uterine levels of COX-2 are necessary for the onset of labor[18,19]. The docking studies performed in our research work clearly indicate the greater binding efficacy of xanthone derivatives over the standard drug celecoxib. While celecoxib showed a docking score of -9.94 kcal/mol. The ligands we designed for study showed a docking score lower than celecoxib. Some ligands like **B1**, **B3**, **B4** and **B5** showed binding score lower than -12 kcal/mol. Synthesis of these compounds produced greater yields as compared to other compounds and physico-chemical characterization clearly established correct identity of the compounds. Hence selective xanthone derivatives can prove to have better ligand binding efficacy and hence better *in vivo* activity than available NSAIDS. After docking study we synthesized these compounds and characterized by different analytical method. Analytical data proved the confirmation of synthesized compound.

Conclusion

In conclusion, it can be said that 3,6-*bis*(3'-substituted propoxy)xanthone derivatives may act as COX-2 inhibitors on the basis of molecular docking runs which contribute to the possible mechanism of anti inflammatory activity of these analogues. These molecules were energetically proficient enough to make stable contacts with target protein on account of effective hydrogen bond and π-cation interactions, which was also supplemented through scoring parameters. In the light of above observation, xanthone derivatives can act as a lead towards the development of potential COX-2 inhibitors, these compounds show excellent correlation between docking results and synthetic data. A considerable amount of work is still required in this direction and is in progress. It will be reported subsequently in future. Further research can be carried out on these compounds and used for testing *in vivo* antiinflammatory activity.

ACKNOWLEDGEMENTS

The authors gratefully acknowledge to Department of Pharmaceutical Sciences, Dibrugarh University, Dibrugarh, India for providing the research facilities.

REFERENCES

1. M. Filizola, J.J. Perez, A. Palomer and D.J. Mauleón, *Mol. Graph. Model*, **15**, 290 (1997).
2. K. Rask, Y. Zhu, W. Wang, L. Hedin and K. Sundfeldt, *Mol. Cancer*, **5**, 62 (2006).
3. D. Coon, A. Gulati, C. Cowan and J.J. He, *J. Endod.*, **33**, 432 (2007).
4. D.E. Furst, *Semin. Arthritis Rheum.*, **26**, 21 (1997).
5. G. Dannhardt and W. Kiefer, *Eur. J. Med. Chem.*, **36**, 109 (2001).
6. B.S.P. Herbert and S.B. Baraf, *Curr. Pharm. Des.*, **13**, 2228 (2007).
7. Y. Sugita, H. Komatani, K. Ohshima, M. Shigemori and A. Nakashima, *Oncol. Rep.*, **18**, 617 (2007).
8. F.L. Lanza, *Am. J. Gastroenterol.*, **93**, 2037 (1998).
9. G. Singh and D.R. Ramey, *J. Rheumatol.*, **51**, 8 (1998).
10. F.E. Silverstein, G. Faich, J.L. Goldstein, L.S. Simon, T. Pincus, A. Whelton, R. Makuch, G. Eisen, N.M. Agrawal, W.F. Stenson, A.M. Burr, W.W. Zhao, J.D. Kent, J.B. Lefkowith, K.M. Verburg and G.S. Geis, *JAMA*, **284**, 1247 (2000).
11. M.I. Chung, J.R. Weng, J.P. Wang, C.M. Teng and C.N. Lin, *Planta Med.*, **68**, 25 (2002).
12. G.M. Morris, R. Huey, W. Lindstrom, M.F. Sanner, R.K. Belew, D.S. Goodsell and A.J. Olson, *J. Comput. Chem.*, **30**, 2785 (2009).
13. M.W. Chang, C. Ayeni, S. Breuer and B.E. Torbett, *PLoS ONE*, **5**, e11955 (2010).
14. H. Park, J. Lee and S. Lee, *Proteins*, **65**, 549 (2006).
15. J.X. Kelly, R. Winter, D.H. Peyton, D.J. Hinrichs and M. Riscoe, *Antimicrob. Agents Chemother.*, **46**, 144 (2002).
15. A.C. Micheletti, N.K. Honda, D.P. Lima, A. Beatriz, M.R. Sant'ana, N.C.P. Carvalho, M.F.C. Matos, L.M.M. Queiróz, D. Bogo and J.R. Zorzatto, *Quim. Nova*, **34**, 1014 (2011).
16. E. Sousa, A. Paiva, N. Nazareth, L. Gales, A.M. Damas, M.S. Nascimento and M. Pinto, *Eur. J. Med. Chem.*, **44**, 3830 (2009).
17. M. Varache-Lembège, S. Moreau, S. Larrouture, D. Montaudon, J. Robert and A. Nuhrich, *Eur. J. Med. Chem.*, **43**, 1336 (2008).
18. S.G. Morham, R. Langenbach, C.D. Loftin, H.F. Tiano, N. Vouloumanos, J.C. Jennette, J.F. Mahler, K.D. Kluckman, A. Ledford, C.A. Lee and O. Smithies, *Cell*, **83**, 473 (1995).
19. I. Chakraborty, S.K. Das, J. Wang and S.K. Dey, *J. Mol. Endocrinol.*, **16**, 107 (1996).